ACSNANO
www.acsnano.org
ARTICLE

Radio Frequency Transistors Using Aligned Semiconducting Carbon Nanotubes with Current-Gain Cutoff Frequency and Maximum Oscillation Frequency Simultaneously Greater than 70 GHz

Yu Cao,[†,⊥] Gerald J. Brady,[‡,⊥] Hui Gui,[§] Chris Rutherglen,[∥] Michael S. Arnold,[‡] and Chongwu Zhou*[,†,§]

[†]Department of Electrical Engineering, University of Southern California, Los Angeles, California 90089, United States
[‡]Department of Materials Science and Engineering, University of Wisconsin—Madison, Madison, Wisconsin 53706, United States
[§]Department of Chemical Engineering and Materials Science, University of Southern California, Los Angeles, California 90089, United States
[∥]Carbonics Inc., Marina del Rey, California 90292, United States

Supporting Information

ABSTRACT: In this paper, we report record radio frequency (RF) performance of carbon nanotube transistors based on combined use of a self-aligned T-shape gate structure, and well-aligned, high-semiconducting-purity, high-density polyfluorene-sorted semiconducting carbon nanotubes, which were deposited using dose-controlled, floating evaporative self-assembly method. These transistors show outstanding direct current (DC) performance with on-current density of 350 μA/μm, transconductance as high as 310 μS/μm, and superior current saturation with normalized output resistance greater than 100 k$\Omega\cdot\mu$m. These transistors create a record as carbon nanotube RF transistors that demonstrate both the current-gain cutoff frequency (f_t) and the maximum oscillation frequency (f_{max}) greater than 70 GHz. Furthermore, these transistors exhibit good linearity performance with 1 dB gain compression point (P_{1dB}) of 14 dBm and input third-order intercept point (IIP_3) of 22 dBm. Our study advances state-of-the-art of carbon nanotube RF electronics, which have the potential to be made flexible and may find broad applications for signal amplification, wireless communication, and wearable/flexible electronics.

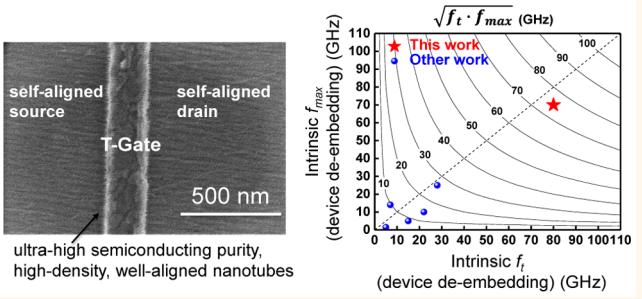

KEYWORDS: *carbon nanotubes, aligned, polyfluorene-sorted, radio frequency, self-aligned T-shape gate, record RF performance, 70 GHz, linearity*

Carbon nanotubes (CNTs) have been a star in the research field for more than two decades. Their prominent characteristics, for example, small size, ballistic transportation, high carrier mobility, and small intrinsic capacitance,[1−5] have been revealed, leading to explosive explorations of utilizing CNTs for next-generation electronics. In terms of digital electronics, researchers have devoted their efforts to replacing silicon with CNTs for sub-10 nm electronics.[6,7] Logic components for integrated digital systems, such as inverters, NAND gates, NOR gates, flip−flops, multiplexers, memories, and computers have been demonstrated.[8−13] In regard to macroelectronics, researchers have devoted their efforts to integrating CNT thin-film transistors (TFTs) with sensors, displays, etc., to achieve large-area and low-cost electronics with added or improved functionalities (e.g., flexibility, stretchability, and lightweight).[14−21] Moreover, printing technologies have been incorporated into CNT electronics, which bring a number of benefits to both the CNT and the printed electronics research areas.[22−25] In addition to digital and macroelectronics, CNTs are especially suitable for radio frequency (RF) electronics because of their high mobility and small intrinsic capacitance and have been extensively investigated as the channel materials for RF transistors since the demonstration of CNT RF transistors in

Received: April 8, 2016
Accepted: June 14, 2016

DOI: 10.1021/acsnano.6b02395
ACS Nano XXXX, XXX, XXX−XXX

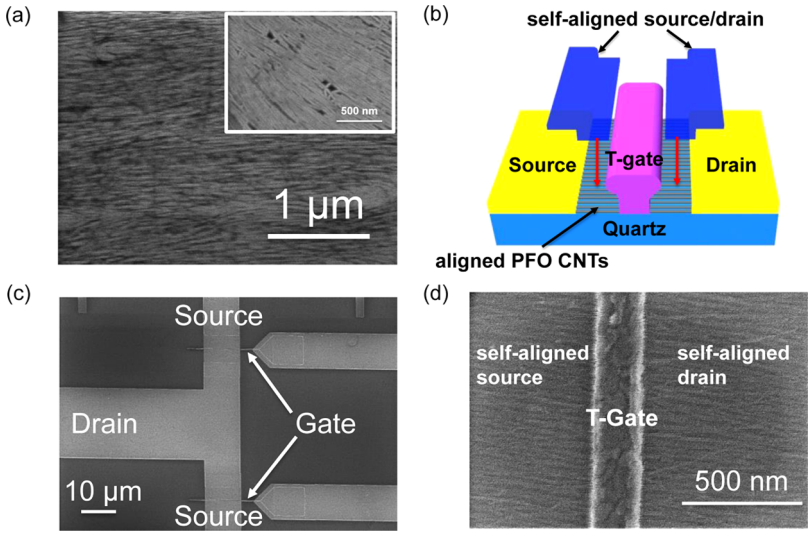

Figure 1. Characterization of the self-aligned T-shape gate transistors based on aligned polyfluorene-sorted CNTs. (a) SEM image of an aligned polyfluorene-sorted CNT film on a quartz substrate. The inset shows another aligned polyfluorene-sorted CNT film prepared by the same method on a Si/SiO_2 substrate to demonstrate the packing density. The packing density is ~40 nanotubes/μm. (b) Schematic of the self-aligned T-shape gate transistor structure. (c) SEM image of an as-fabricated self-aligned T-shape gate transistor. (d) Zoomed-in SEM image of a channel region. The T-shape gate, self-aligned source and drain, and aligned polyfluorene-sorted CNTs underneath are clearly demonstrated.

2004,[26−36] and CNT-based high-performance RF circuits have been demonstrated.[37−39]

CNTs can exist as either aligned arrays or networks as the channel materials for RF transistors. In terms of aligned arrays, there are two major approaches to get aligned CNTs. One approach is to directly synthesize aligned CNTs via chemical vapor deposition (CVD).[35,40−43] Aligned CNTs with a density as high as 130 nanotubes/μm have been achieved.[35] However, the semiconducting purity of CVD-aligned CNTs with high density is usually ~60%. Such a semiconducting purity would lead to degraded current saturation of RF transistors, which deteriorates the RF performance, especially the power gain frequency response. Semiconducting purity of CVD-aligned CNTs can be improved as high as ~95%.[40,42] However, the reported work usually had rather low nanotube density, leading to degraded on-current density and transconductance. Moreover, even the ~95% semiconducting purity is still far from the ideal to achieve good current saturation. RF transistors based on CVD-aligned CNTs have been reported by several research groups and show maximum oscillation frequency (f_{max}) below 15 GHz, which is usually much lower than their current-gain cutoff frequency (f_t) due to the nonideal current saturation.[31,33−35] The other approach to achieve aligned CNTs is to carry out postsynthesis sorting and assembly. RF transistors based on dielectrophoresis (DEP)-aligned CNTs have been reported with this approach.[27,32] With semiconducting purity of ~99.6%, the RF performance (especially the f_{max}) of these DEP-aligned nanotube transistors improves in comparison with the transistors based on CVD-aligned CNTs.[32] Unfortunately, there still exist residual metallic CNTs due to the limitation of sorting methods and organizational disorder due to the limitation of assembly methods. As a result, the RF performance of these aligned CNT transistors still shows a big difference between f_t and f_{max}, and the f_{max}, which is of key importance for practical applications, so far has not exceeded 30 GHz.[32] In terms of CNT networks, they are usually achieved by dispersing presorted CNT solutions onto target substrates. The presorted CNT solutions usually have a higher semiconducting purity compared with CVD-synthesized CNTs. One method to achieve presorted CNT solutions with high semiconducting purity is through density gradient ultracentrifugation (DGU).[44,45] Several research groups have reported RF performance of CNT transistors based on DGU-sorted high-semiconducting-purity CNT networks.[28−30] However, due to the still less-than-ideal semiconducting purity and the existence of tube−tube junctions, the RF performance of these transistors is worse than that of the transistors based on CVD-aligned nanotubes. Another method to achieve high-semiconducting-purity presorted CNT solutions is through polymer separation.[46,47] The semiconducting purity of presorted CNT solutions based on polyfluorene separation can exceed 99.9%, which is a remarkable improvement compared with other separation methods.[48] RF transistors based on polyfluorene-sorted CNT networks have successfully advanced the RF performance of the network-based nanotube RF transistors to the level of the best aligned-nanotube-based RF transistors.[36]

Based on the extraordinary performance of the RF transistors using polyfluorene-sorted CNT networks, it is foreseen that the RF performance of transistors based on aligned polyfluorene-sorted CNTs should be even better. With the ultrahigh semiconducting purity and the removal of tube−tube junctions, excellent transconductance and current saturation, both of which are particularly important for RF transistors, can be expected. Recently, a method named dose-controlled, floating evaporative self-assembly (DFES) has been developed by Joo, Brady et al. to achieve aligned polyfluorene-sorted CNTs over large areas, which provides an excellent platform for CNT RF electronics.[49−51]

In this paper, we report record RF performance of CNT transistors based on combined use of a self-aligned T-shape gate structure, and well-aligned, high-semiconducting-purity, high-density polyfluorene-sorted semiconducting carbon nanotubes. These transistors show excellent direct current (DC) performance, with on-current density of 350 μA/μm, transconductance as high as 310 μS/μm, and superior current saturation with normalized output resistance greater than 100

DOI: 10.1021/acsnano.6b02395
ACS Nano XXXX, XXX, XXX−XXX

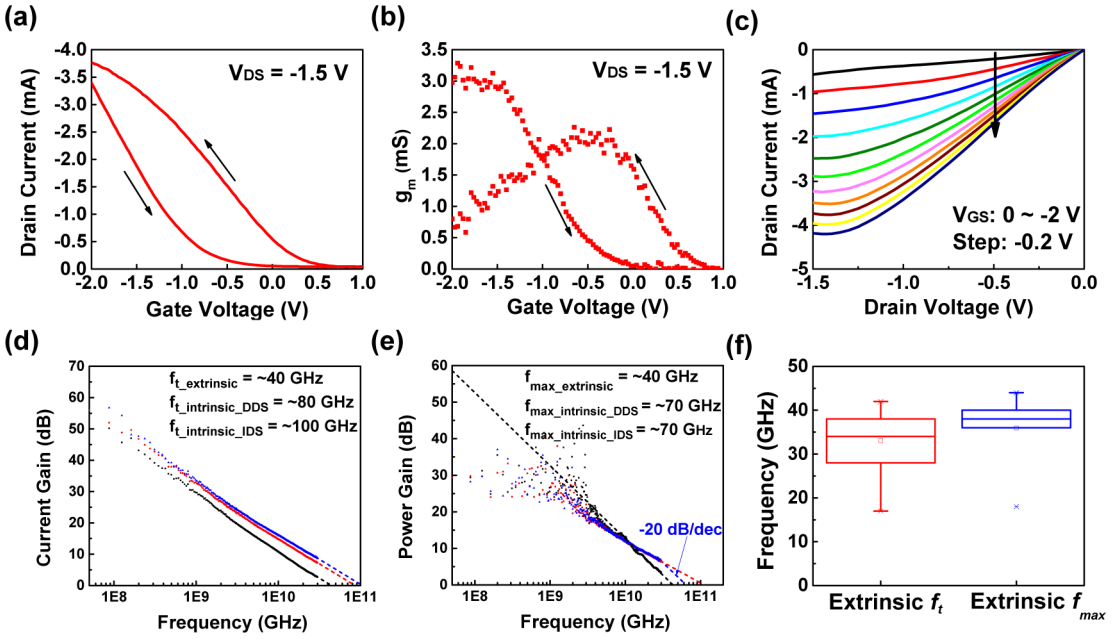

Figure 2. DC and RF characterizations of the self-aligned T-shape gate transistors based on aligned polyfluorene-sorted CNTs. (a) Transfer characteristic (I_{DS}–V_{GS} curve) of a representative CNT transistor at V_{DS} = −1.5 V. The channel width (W) is 10 μm. (b) Transconductance (g_m–V_{GS} curve) of the same transistor in panel a. (c) Output characteristics (I_{DS}–V_{DS} curves) of the same transistor in panel a at various V_{GS} from 0 to −2 V with a step of −0.2 V. (d) Extrinsic and intrinsic current–gain frequency response. (e) Extrinsic and intrinsic power gain frequency response. (f) Statistics of the extrinsic RF performance of 23 aligned polyfluorene-sorted CNT transistors.

kΩ·μm. (The normalized output resistance is defined as the change in the drain-to-source voltage over the change in the drain-to-source current multiplied by the channel width in the current saturation region, and reflects the quality of current saturation. A better current saturation will yield a larger normalized output resistance.) In regard to the RF performance, these transistors create a record as CNT transistors that exhibit both f_t and f_{max} greater than 40 GHz (before de-embedding) and 70 GHz (after de-embedding). In addition, these transistors based on aligned polyfluorene-sorted CNTs demonstrate good linearity behavior with 1 dB gain compression point (P_{1dB}) of 14 dBm, and input third-order intercept point (IIP_3) of 22 dBm. Our study advances state-of-the-art of CNT RF electronics and further accelerates the applications of CNT RF transistors in complex circuits and systems.

RESULTS AND DISCUSSION

Aligned polyfluorene-sorted CNTs on quartz substrates, achieved by DFES (Methods section), were used as the channel material for RF transistors. Figure 1a shows a scanning electron microscope (SEM) image of an aligned polyfluorene-sorted CNT film on a quartz substrate. Aligned polyfluorene-sorted CNTs with high density can be clearly seen from the SEM image. However, it is difficult to find out the exact packing density on quartz substrates due to the charging effects. We prepared another aligned polyfluorene-sorted CNT film on a Si/SiO_2 substrate with the same method to determine the packing density. The SEM image of the aligned polyfluorene CNTs on the Si/SiO_2 substrate is shown in the inset of Figure 1a. The packing density of the aligned polyfluorene-sorted CNTs is ~40 nanotubes/μm. We then fabricated RF transistors based on the aligned CNT film with a self-aligned T-shape gate structure. Figure 1b delineates a schematic of the self-aligned T-shape gate structure. The device structure has been widely used in III–V and Si devices and applied to carbon nanotube research field in our previously reported work.[30,31,36,52] The self-aligned T-shape gate structure has the advantages of reducing parasitic capacitance, decreasing gate resistance, scaling down channel length, and offering optimized gate control. Figure 1c presents a SEM image of an as-fabricated self-aligned T-shape gate transistor. The details of the device fabrication process can be found in the Methods section. Figure 1d shows a zoomed-in SEM image of a channel region. The T-shape gate, self-aligned source and drain, and aligned polyfluorene-sorted CNTs underneath are clearly demonstrated. The channel length (L) of the RF transistors is ~100 nm, and the ungated region on each side of the T-shape gate is ~10–20 nm. In addition to devices on rigid substrates, the T-shape gate RF transistors have great potential to be made on flexible substrates,[9,21] which brings promising applications such as wearable/flexible electronics for our devices.

DC performance of the as-fabricated RF transistors based on the aligned polyfluorene-sorted CNTs are characterized. Figure 2a presents the transfer characteristics of a representative transistor with a channel width (W) of 10 μm at a drain-to-source bias (V_{DS}) of −1.5 V. The transfer curve shows a p-type transistor behavior with hysteresis of ~1 V. The on-current density is ~350 μA/μm measured at a gate-to-source bias (V_{GS}) of −2 V, which corresponds to ~9 μA/nanotube. This on-current density is the highest among all CNT RF transistors reported so far.[31,32,35,36] The off-current density is ~4 μA/μm measured at V_{GS} = 0.82 V, which corresponds to 0.1 μA/nanotube. The on/off ratio is ~90, which improves significantly compared with that of the transistors based on CVD-aligned CNTs.[31,33−35] As discussed above, CVD-aligned CNTs are a mixture of metallic and semiconducting CNTs, while the aligned polyfluorene-sorted CNTs by the DFES method are of ultrahigh semiconducting purity, which leads to the improved on/off ratio. However, the on/off ratio is much lower than the

DOI: 10.1021/acsnano.6b02395
ACS Nano XXXX, XXX, XXX–XXX

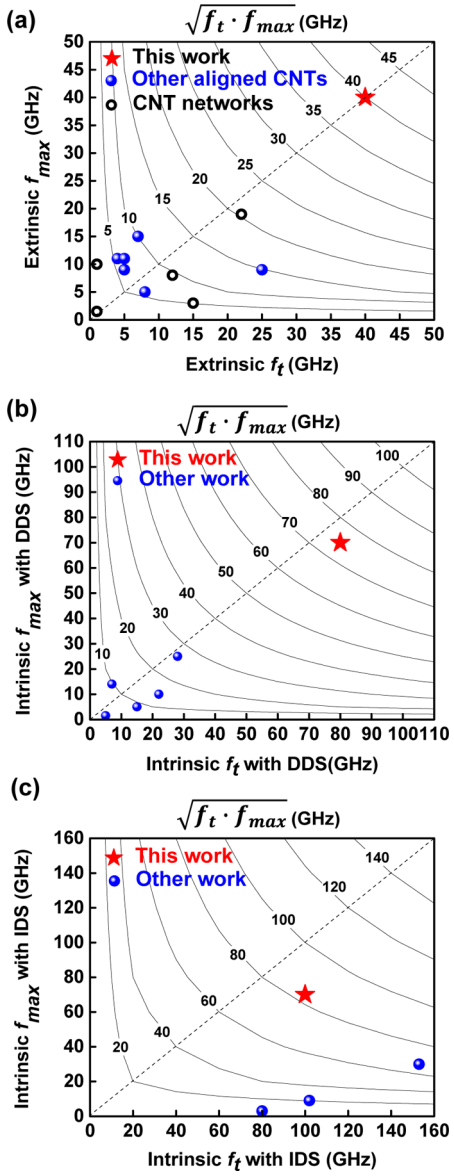

Figure 3. Comparison of the RF performance between different carbon nanotube transistors. (a) Comparison of the extrinsic frequency response between this work, other work based on aligned CNTs, and other work based on CNT networks. (b) Comparison of the intrinsic frequency response with the device de-embedding structure (DDS, Supporting Information Figure S2) between this work and other work. (c) Comparison of the intrinsic frequency response with the intrinsic de-embedding structure (IDS, Supporting Information, Figure S3) between this work and other work.

values of the field-effect transistors (FETs) based on nanotubes prepared with the same DFES method in literature.[49] We noticed that the values of the on/off ratio in literature were achieved from FETs with smaller source-to-drain biases and longer channel lengths. We measured the transfer curves of another representative nanotube RF transistor and extracted the corresponding on/off ratio under various V_{DS} from −0.1 to −1.6 V with a step of −0.3 V (Supporting Information, Figure S1). The on/off ratio decreases from ∼2000 to ∼50 with the increase of V_{DS} from −0.1 to −1.6 V, suggesting that the low on/off ratio for the T-gate RF transistors measured at V_{DS} = −1.5 V might be caused by the drain-induced barrier lowering (DIBL) effect. Fortunately, the on/off ratio has no direct relation with the frequency response for RF transistors. The transconductance of the polyfluorene-sorted CNT RF transistors in Figure 2a is extracted and plotted in Figure 2b. We can observe that the peak transconductance is ∼310 μS/μm for the forward sweep and ∼210 μS/μm for the backward sweep. The transconductance of the aligned polyfluorene-sorted CNT RF transistors is also the best among all CNT transistors reported so far. It improves by a factor of ∼6 compared with the previously reported best transconductance for aligned CNT RF transistors[31−33] and by a factor of ∼8 compared with the best transconductance for RF transistors based on CNT networks.[36] Current saturation is another important aspect for RF transistors. The output characteristics of the same transistor in Figure 2a are shown in Figure 2c. We can observe that drain current (I_D) starts to saturate when V_{DS} goes beyond −1.3 V under various gate biases from 0 to −2 V. The normalized output resistance is extremely large, as one can observe that the output curves are essentially flat when V_{DS} goes beyond −1.4 V for various V_{GS} (−0.8 − −2 V). The normalized output resistance is conservatively estimated to be greater than 100 kΩ·μm, which is greatly improved in comparison with transistors based on CVD-aligned CNTs[31,33−35] and comparable to the best value reported for transistors based on CNT networks.[36] On the basis of the excellent transconductance and current saturation, we expect to achieve record RF performance for our transistors based on aligned polyfluorene-sorted CNTs.

The RF performance of the self-aligned T-shape gate transistors based on aligned polyfluorene-sorted CNTs are then characterized. Vector network analyzer (N5242A PNA-X) and microprobes, with ground−signal−ground (GSG) structure and a pitch of 150 μm, were utilized to measure the S-parameters. Before the measurement, we calibrated the entire setup with short-open-load-through (SOLT) standards. S-parameters were then measured for the RF transistors from 50 MHz to 30 GHz, and the corresponding current-gain (h_{21}) and the unilateral power gain (U) were extracted. We also measured on-chip open and short structures for the de-embedding process. We note that there exist two de-embedding structures for CNT RF transistors in literature.[27−32,34−36] One de-embedding structure would remove only the parasitics from the bonding pads without removing the capacitances associated with the gate. This de-embedding structure would reveal the performance of RF transistors achievable for practical applications (e.g., the RF transistors can be integrated into RF circuits and systems without the bonding pads) and is therefore widely used in semiconductor research.[29,30,34−36] For clarity, we name this de-embedding structure as the device de-embedding structure (DDS), and the schematic of this structure is shown in the Supporting Information Figure S2. The other de-embedding structure would remove both the parasitics from the bonding pads and the fringe capacitances associated with the gate and reveal the intrinsic performance upper-limit of material properties.[27,28,31,32] However, the de-embedded performance using this de-embedding structure is not achievable in practical applications, because the fringe capacitances of the gate are part of the RF transistors and cannot be eliminated. For clarity, we name this de-embedding structure as the intrinsic de-embedding structure (IDS), and the schematic of this structure is shown in the Supporting Information Figure S3. In this work, we de-embed the measured S-parameters with both DDS and IDS. Figure 2d,e shows the current-gain and power gain frequency response of a

DOI: 10.1021/acsnano.6b02395
ACS Nano XXXX, XXX, XXX−XXX

Table 1. Comparison of RF Performance between CNTs, graphene, MoS_2 and black phosphorus transistors

Reference	Materials		Channel length (nm)	Extrinsic f_t (GHz)	Extrinsic f_{max} (GHz)	Intrinsic f_t with DDS (GHz)	Intrinsic f_{max} with DDS (GHz)	Intrinsic f_t with IDS (GHz)	Intrinsic f_{max} with IDS (GHz)
This Work	DFES aligned CNTs		100	40	40	80	70	100	70
27	DEP aligned CNTs		300	4	-	11	-	30	-
28	CNT networks		300	15	3	-	-	80	3
29	CNT networks		500	1	1.5	5	1.5	-	-
30	CNT networks	Si/SiO_2	140	1	10	22	10	-	-
		quartz		12	8				
31	CVD aligned CNTs		140	25	9	-	-	102	9
32	DEP aligned CNTs		100	7	15	-	-	153	30
33	CVD aligned CNTs		700	5	9	-	-	-	-
34	CVD aligned CNTs		500	8	5	15	5	-	-
35	CVD aligned CNTs		1200	5	11	7	14	-	-
36	CNT networks		120	22	19	28	25	-	-
54	graphene		240	55	10	-	-	100	10
55	graphene		250	15	18	-	-	-	-
56	graphene		100	41	38	-	-	110	70
57	MoS_2		68	10	15	-	-	42	50
58	black phosphorus		300	8	12	12	20	-	-

representative aligned polyfluorene-sorted CNT RF transistor with a channel width of 2 × 10 μm. The transistor was biased at V_{DS} = −1.5 V and V_{GS} = −1.2 V. The extrinsic f_t and f_{max} are ∼40 and ∼40 GHz, respectively. The intrinsic f_t and f_{max} with DDS are ∼80 and ∼70 GHz, respectively, and the intrinsic f_t and f_{max} with IDS are ∼100 and ∼70 GHz, respectively. We note that the intrinsic unilateral power gain did not demonstrate the theoretical slope of −20 dB/dec even at the highest measuring frequency of 30 GHz. The range of the intrinsic f_{max} is estimated between 60−100 GHz via curve-fitting with two different slopes (the theoretical slope of −20 dB/dec and the exhibited slope of approximately −10 dB/dec), and the use of 70 GHz is a conservative estimation of the intrinsic f_{max}. In order to demonstrate the uniformity of our aligned polyfluorene-sorted CNT RF transistors, we carried out a statistical study of 23 devices. Figure 2f presents the statistics of the extrinsic performance of the 23 devices. The extrinsic f_t is 32.5 ± 6.9 GHz, and the extrinsic f_{max} is 35.3 ± 7.7 GHz. The standard deviations of both f_t and f_{max} are ∼20% of their average values, which may be caused by the variations of nanotubes across the substrates, the variations of the self-aligned T-shape gate fabrication process, and the variations of contact resistance.[53] In addition, one can observe that the extrinsic f_{max} is consistently larger than the extrinsic f_t, which is preferable for practical applications and further confirms that our transistors have good current saturation.

Our aligned polyfluorene-sorted CNT RF transistors advance the state-of-the-art of CNT RF transistors. In terms of the extrinsic RF performance, our aligned polyfluorene-sorted CNT transistors create a record as CNT RF transistors that demonstrate both f_t and f_{max} of ∼40 GHz. Figure 3a plots the extrinsic f_t and f_{max} for representative reported CNT RF transistors (including transistors based on aligned CNTs and CNT networks). We can observe that the extrinsic f_t, the extrinsic f_{max} and the geometric mean of f_t and f_{max} for our aligned polyfluorene-sorted CNT transistors are all ∼40 GHz and outperform all the other CNT RF transistors. In terms of the intrinsic RF performance, our transistors are also the best among all CNT RF transistors. Figure 3b shows the comparison of the intrinsic RF performance with DDS between this work and other work. Our work is the best with the geometric mean of f_t and f_{max} of ∼70 GHz. In comparison, the geometric mean of f_t and f_{max} for other CNT RF transistors does not exceed 30 GHz. Figure 3c presents the comparison of the intrinsic RF performance with IDS between this work and other work. The f_{max} and the geometric mean of f_t and f_{max} for our CNT transistors with IDS is remarkably higher than that of the other CNT transistors. For practical applications, RF transistors cannot operate beyond the frequency of f_{max} in order to have a power gain greater than one. Our transistors have an intrinsic f_{max} at least 2× larger compared with all the other nanotube RF transistors and a smaller difference between the

DOI: 10.1021/acsnano.6b02395
ACS Nano XXXX, XXX, XXX−XXX

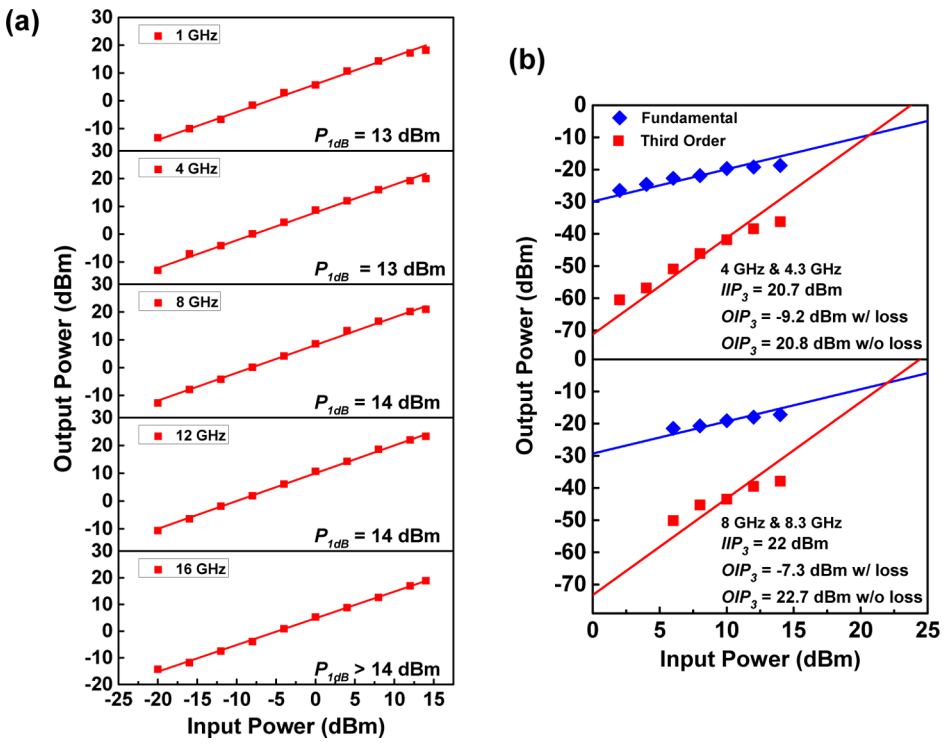

Figure 4. Linearity performance of the self-aligned T-shape gate transistors based on aligned polyfluorene-sorted CNTs. (a) Output power vs input power curves for the single-tone test at frequencies of 1, 4, 8, 12, and 16 GHz. (b) Output power vs input power of the fundamental term and the third-order term in the frequency range of 4 and 8 GHz for the two-tone test.

intrinsic f_t and f_{max}, both of which make our transistors more favorable for practical applications. Moreover, we note that the intrinsic performance of our aligned polyfluorene-sorted CNT transistors with IDS is similar to that with DDS, further confirming the advantages of our self-aligned T-shape gate structure. Table 1 lists the detailed RF performance of all the CNT transistors in comparison, and also includes RF performance of representative graphene,[54−56] MoS_2,[57] and black phosphorus transistors.[58] One can observe that the RF performance of our aligned polyfluorene-sorted CNT transistors is comparable to the best RF performances so far reported for graphene RF transistors but with significantly better current saturation, which is important for amplification applications,[54−56] and exceeds the RF performance of MoS_2[57] and black phosphorus RF transistors.[58]

Linearity performance is also important for RF transistors. P_{1dB} and IIP_3 are the two parameters to characterize the linearity performance of RF transistors. Single-tone and two-tone tests are often used to measure the two parameters. The detailed setup for the single-tone and two-tone tests can be found in our previous work.[36] Figure 4a plots the results of the single-tone test at different frequencies of 1, 4, 8, 12, and 16 GHz. With linear fitting at low input power levels, the P_{1dB} for the aligned polyfluorene-sorted CNT RF transistors is extracted to be 13−14 dBm. One thing to note is that we partially de-embedded out the losses from the wires and connectors of the measurement system with the single-tone test of the on-chip short structure (Supporting Information Figure S2). Details for the de-embedding process of the single-tone test can be found in the Supporting Information (Figure S4). We can observe that there are power gains for the CNT transistors at various measurement frequencies even without input and output impedance matching. The power gain is ∼8 dB, corresponding well with the power gain frequency response (Figure 2e). Figure 4b shows the results of the two-tone test at frequency ranges of 4 and 8 GHz. The IIP_3 is 20.7 and 22 dBm for 4 and 8 GHz, respectively. The corresponding output third-order intercept point (OIP_3) for 4 and 8 GHz, respectively, is −9.2 and −7.3 dBm with losses from wires and connectors and 20.8 and 22.7 dBm, respectively, after partially de-embedding out the losses from wires and connectors. The linearity performance of the aligned polyfluorene-sorted CNT transistors is comparable to that of CVD-aligned CNT transistors[31] and improved compared with that of the transistors based on CNT networks.[30,36]

CONCLUSION

In summary, we have made self-aligned T-shape gate RF transistors based on aligned polyfluorene-sorted CNTs. Excellent DC performance, with on-current density of 350 μA/μm, transconductance as high as 310 μS/μm, and superior current saturation with normalized output resistance greater than 100 k$\Omega\cdot\mu$m, is achieved for these aligned polyfluorene-sorted CNT transistors. Besides, these aligned polyfluorene-sorted transistors show record RF performance. Extrinsic f_t and f_{max} are ∼40 and ∼40 GHz, respectively. Intrinsic f_t and f_{max} with device de-embedding structure are ∼80 and ∼70 GHz, respectively, and intrinsic f_t and f_{max} with intrinsic de-embedding structure are ∼100 and ∼70 GHz, respectively. These aligned polyfluorene-sorted CNT transistors demonstrate both f_t and f_{max} greater than 70 GHz. In addition, these RF transistors based on aligned polyfluorene-sorted CNTs show ∼20% device-to-device variations. Moreover, these CNT RF transistors also demonstrate good linearity performance, which is important for their practical applications. Our study pushes forward the frontiers of CNT RF electronics and is very

DOI: 10.1021/acsnano.6b02395
ACS Nano XXXX, XXX, XXX−XXX

meaningful and encouraging for the field of CNT RF electronics. Moreover, the carbon nanotube devices, which have the potential to be made flexible, may find broad applications for signal amplification, wireless communication, and wearable/flexible electronics.

METHODS

Preparation of Aligned CNT Films. Large-diameter semiconducting enriched CNTs are extracted from arc discharge carbon nanotube powder (Aldrich, 750514) using the CNT dispersant poly[(9,9-dioctylfluorenyl-2,7-diyl)-*alt-co*-(6,6′-{2,2′-bipyridine})] (American Dye source, ADS153UV) (PFO-BPy), which selectively wraps purely semiconducting CNTs. After the initial semiconducting sorting and polymer washing steps (details provided elsewhere[49]), the PFO-BPy wrapped CNTs are dispersed in chloroform to a concentration of 10 μg/mL. To perform DFES alignment, the CNT ink is spread onto a water subphase using a syringe pump to supply discrete approximately microliter doses. Simultaneously, a partially submerged quartz substrate is pulled out of the aqueous subphase at constant lift rate. Each dose of ink spreads on the water due to surface tension effects and wets the surface of the receiving substrate creating a thin film of ink along the width of the substrate−water meniscus. Each respective dose results in an approximately 100 μm tall band of aligned CNTs that spans the width of the substrate. Nearly full surface coverage of aligned CNTs is achieved by tuning the lift and dose rate such that sequential bands are placed directly next to one another with minimal overlap.

CNT Film Surface Treatment. Following alignment, the CNT films undergo surface treatments (unpublished data). In brief, the samples are rinsed in a toluene bath at 60 °C for 1 h, then transferred into an isopropyl bath for 30 s, followed by blow drying in an air stream. Finally the films are annealed in a tube furnace in vacuum at a base pressure of 4×10^{-6} Torr at a temperature of 400 °C for 1 h.

Fabrication of Self-Aligned T-Shape Gate RF Transistors Based on Aligned Polyfluorene-Sorted CNTs. Aligned polyfluorene-sorted CNTs on quartz substrates, achieved by dose-controlled, floating evaporative self-assembly method (DFES), were used as the channel material. Alignment markers were patterned followed by identifying the aligned regions with SEM. The CNTs outside the device channel regions were etched away by oxygen plasma. Source and drain electrodes (1/50 nm thickness of titanium/gold) were then patterned. Sequentially, an aluminum T-shape gate (~140 nm thickness) was patterned by electron beam lithography and oxidized in air at 120 °C. Finally, 10 nm thickness of palladium was deposited as the self-aligned source and drain contacts.

ASSOCIATED CONTENT

Supporting Information

The Supporting Information is available free of charge on the ACS Publications website at DOI: 10.1021/acsnano.6b02395.

Transfer curves of self-aligned T-shape gate nanotube radio frequency (RF) transistors under various drain-to-source biases, device de-embedding structure, intrinsic de-embedding structure, and de-embedding process for the two-tone test (PDF)

AUTHOR INFORMATION

Corresponding Author

*chongwuz@usc.edu.

Author Contributions

⊥Y.C. and G.J.B. contributed equally to this work.

Notes

The authors declare the following competing financial interest(s): C.Z. is a founder, shareholder, and consultant to Carbonics Inc., and C.R. is employed by Carbonics Inc., which focuses on commercializing carbon-nanotube-based radio frequency electronics.

ACKNOWLEDGMENTS

We would like to acknowledge the collaboration of this research with King Abdul-Aziz City for Science and Technology (KACST) via The Center of Excellence for Nanotechnologies (CEGN). We also acknowledge the Center for High Frequency Electronics (CHFE) at UCLA for technical support. We thank Mr. Minji Zhu at CHFE for help with RF measurements. We also thank Dr. Kosmas Galatsis at Carbonics Inc. for helpful discussions. G.J.B. and M.S.A. acknowledge support from the National Science Foundation Grant No. CMMI-1462771 and Air Force Contract No. FA8750-15-C-0257. G.J.B. also acknowledges support from a National Science Foundation Graduate Research Fellowship.

REFERENCES

(1) Saito, R.; Dresselhaus, G.; Dresselhaus, M. S. *Physical Properties of Carbon Nanotubes*; Imperial College Press: London, 1998; Vol. 35, pp 73−81.

(2) Javey, A.; Guo, J.; Wang, Q.; Lundstrom, M.; Dai, H. J. Ballistic Carbon Nanotube Field-Effect Transistors. *Nature* **2003**, *424*, 654−657.

(3) Zhou, X.; Park, J. Y.; Huang, S.; Liu, J.; McEuen, P. L. Band Structure, Phonon Scattering, and the Performance Limit of Single-Walled Carbon Nanotube Transistors. *Phys. Rev. Lett.* **2005**, *95*, 146805.

(4) Rutherglen, C.; Jain, D.; Burke, P. Nanotube Electronics for Radiofrequency Applications. *Nat. Nanotechnol.* **2009**, *4*, 811−819.

(5) Durkop, T.; Getty, S. A.; Cobas, E.; Fuhrer, M. S. Extraordinary Mobility in Semiconducting Carbon Nanotubes. *Nano Lett.* **2004**, *4*, 35−39.

(6) Franklin, A. D.; Luisier, M.; Han, S. J.; Tulevski, G.; Breslin, C. M.; Gignac, L.; Lundstrom, M. S.; Haensch, W. Sub-10 nm Carbon Nanotube Transistor. *Nano Lett.* **2012**, *12*, 758−762.

(7) Cao, Q.; Han, S. J.; Tersoff, J.; Franklin, A. D.; Zhu, Y.; Zhang, Z.; Tulevski, G. S.; Tang, J. S.; Haensch, W. End-Bonded Contacts for Carbon Nanotube Transistors with Low, Size-Independent Resistance. *Science* **2015**, *350*, 68−72.

(8) Ryu, K.; Badmaev, A.; Wang, C.; Lin, A.; Patil, N.; Gomez, L.; Kumar, A.; Mitra, S.; Wong, H. S.; Zhou, C. CMOS-Analogous Wafer-Scale Nanotube-on-Insulator Approach for Submicrometer Devices and Integrated Circuits Using Aligned Nanotubes. *Nano Lett.* **2009**, *9*, 189−197.

(9) Cao, Q.; Kim, H. S.; Pimparkar, N.; Kulkarni, J. P.; Wang, C.; Shim, M.; Roy, K.; Alam, M. A.; Rogers, J. A. Medium-Scale Carbon Nanotube Thin-Film Integrated Circuits on Flexible Plastic Substrates. *Nature* **2008**, *454*, 495−500.

(10) Geier, M. L.; McMorrow, J. J.; Xu, W.; Zhu, J.; Kim, C. H.; Marks, T. J.; Hersam, M. C. Solution-Processed Carbon Nanotube Thin-Film Complementary Static Random Access Memory. *Nat. Nanotechnol.* **2015**, *10*, 944−948.

(11) Shulaker, M. M.; Hills, G.; Patil, N.; Wei, H.; Chen, H. Y.; Wong, H. S.; Mitra, S. Carbon Nanotube Computer. *Nature* **2013**, *501*, 526−530.

(12) Ding, L.; Zhang, Z. Y.; Liang, S. B.; Pei, T.; Wang, S.; Li, Y.; Zhou, W. W.; Liu, J.; Peng, L. M. Cmos-Based Carbon Nanotube Pass-Transistor Logic Integrated Circuits. *Nat. Commun.* **2012**, *3*, 677.

(13) Suriyasena Liyanage, L.; Xu, X. Q.; Pitner, G.; Bao, Z. N.; Wong, H. S. P. VLSI-Compatible Carbon Nanotube Doping Technique with Low Work-Function Metal Oxides. *Nano Lett.* **2014**, *14*, 1884−1890.

(14) Zhang, J.; Fu, Y.; Wang, C.; Chen, P. C.; Liu, Z.; Wei, W.; Wu, C.; Thompson, M. E.; Zhou, C. Separated Carbon Nanotube Macroelectronics for Active Matrix Organic Light-Emitting Diode Displays. *Nano Lett.* **2011**, *11*, 4852−4858.

DOI: 10.1021/acsnano.6b02395
ACS Nano XXXX, XXX, XXX−XXX

(15) Takahashi, T.; Yu, Z. B.; Chen, K.; Kiriya, D.; Wang, C.; Takei, K.; Shiraki, H.; Chen, T.; Ma, B. W.; Javey, A. Carbon Nanotube Active-Matrix Backplanes for Mechanically Flexible Visible Light and X-Ray Imagers. *Nano Lett.* **2013**, *13*, 5425−5430.
(16) Wang, C.; Hwang, D.; Yu, Z. B.; Takei, K.; Park, J.; Chen, T.; Ma, B. W.; Javey, A. User-Interactive Electronic Skin for Instantaneous Pressure Visualization. *Nat. Mater.* **2013**, *12*, 899−904.
(17) Chen, H.; Cao, Y.; Zhang, J.; Zhou, C. Large-Scale Complementary Macroelectronics Using Hybrid Integration of Carbon Nanotubes and Igzo Thin-Film Transistors. *Nat. Commun.* **2014**, *5*, 4097.
(18) Wang, H. L.; Li, Y. X.; Jimenez-Oses, G.; Liu, P.; Fang, Y.; Zhang, J.; Lai, Y. C.; Park, S.; Chen, L. W.; Houk, K. N.; Bao, Z. A. N-Type Conjugated Polymer-Enabled Selective Dispersion of Semiconducting Carbon Nanotubes for Flexible CMOS-Like Circuits. *Adv. Funct. Mater.* **2015**, *25*, 1837−1844.
(19) Honda, W.; Harada, S.; Ishida, S.; Arie, T.; Akita, S.; Takei, K. High-Performance, Mechanically Flexible, and Vertically Integrated 3D Carbon Nanotube and Ingazno Complementary Circuits with a Temperature Sensor. *Adv. Mater.* **2015**, *27*, 4674−4680.
(20) Sun, D. M.; Timmermans, M. Y.; Tian, Y.; Nasibulin, A. G.; Kauppinen, E. I.; Kishimoto, S.; Mizutani, T.; Ohno, Y. Flexible High-Performance Carbon Nanotube Integrated Circuits. *Nat. Nanotechnol.* **2011**, *6*, 156−161.
(21) Cao, X.; Cao, Y.; Zhou, C. Imperceptible and Ultraflexible P-Type Transistors and Macroelectronics Based on Carbon Nanotubes. *ACS Nano* **2016**, *10*, 199−206.
(22) Cao, X.; Chen, H.; Gu, X.; Liu, B.; Wang, W.; Cao, Y.; Wu, F.; Zhou, C. Screen Printing as a Scalable and Low-Cost Approach for Rigid and Flexible Thin-Film Transistors Using Separated Carbon Nanotubes. *ACS Nano* **2014**, *8*, 12769−12776.
(23) Vuttipittayamongkol, P.; Wu, F. Q.; Chen, H. T.; Cao, X.; Liu, B. L.; Zhou, C. W. Threshold Voltage Tuning and Printed Complementary Transistors and Inverters Based on Thin Films of Carbon Nanotubes and Indium Zinc Oxide. *Nano Res.* **2015**, *8*, 1159−1168.
(24) Ha, M. J.; Xia, Y.; Green, A. A.; Zhang, W.; Renn, M. J.; Kim, C. H.; Hersam, M. C.; Frisbie, C. D. Printed, Sub-3V Digital Circuits on Plastic from Aqueous Carbon Nanotube Inks. *ACS Nano* **2010**, *4*, 4388−4395.
(25) Lau, P. H.; Takei, K.; Wang, C.; Ju, Y.; Kim, J.; Yu, Z. B.; Takahashi, T.; Cho, G.; Javey, A. Fully Printed, High Performance Carbon Nanotube Thin-Film Transistors on Flexible Substrates. *Nano Lett.* **2013**, *13*, 3864−3869.
(26) Li, S. D.; Yu, Z.; Yen, S. F.; Tang, W. C.; Burke, P. J. Carbon Nanotube Transistor Operation at 2.6 GHz. *Nano Lett.* **2004**, *4*, 753−756.
(27) Le Louarn, A.; Kapche, F.; Bethoux, J. M.; Happy, H.; Dambrine, G.; Derycke, V.; Chenevier, P.; Izard, N.; Goffman, M. F.; Bourgoin, J. P. Intrinsic Current Gain Cutoff Frequency of 30 GHz with Carbon Nanotube Transistors. *Appl. Phys. Lett.* **2007**, *90*, 233108.
(28) Nougaret, L.; Happy, H.; Dambrine, G.; Derycke, V.; Bourgoin, J. P.; Green, A. A.; Hersam, M. C. 80 GHz Field-Effect Transistors Produced Using High Purity Semiconducting Single-Walled Carbon Nanotubes. *Appl. Phys. Lett.* **2009**, *94*, 243505.
(29) Wang, C.; Badmaev, A.; Jooyaie, A.; Bao, M.; Wang, K. L.; Galatsis, K.; Zhou, C. Radio Frequency and Linearity Performance of Transistors Using High-Purity Semiconducting Carbon Nanotubes. *ACS Nano* **2011**, *5*, 4169−4176.
(30) Che, Y.; Badmaev, A.; Jooyaie, A.; Wu, T.; Zhang, J.; Wang, C.; Galatsis, K.; Enaya, H. A.; Zhou, C. Self-Aligned T-Gate High-Purity Semiconducting Carbon Nanotube Rf Transistors Operated in Quasi-Ballistic Transport and Quantum Capacitance Regime. *ACS Nano* **2012**, *6*, 6936−6943.
(31) Che, Y.; Lin, Y. C.; Kim, P.; Zhou, C. T-Gate Aligned Nanotube Radio Frequency Transistors and Circuits with Superior Performance. *ACS Nano* **2013**, *7*, 4343−4350.
(32) Steiner, M.; Engel, M.; Lin, Y. M.; Wu, Y. Q.; Jenkins, K.; Farmer, D. B.; Humes, J. J.; Yoder, N. L.; Seo, J. W. T.; Green, A. A.; Hersam, M. C.; Krupke, R.; Avouris, P. High-Frequency Performance of Scaled Carbon Nanotube Array Field-Effect Transistors. *Appl. Phys. Lett.* **2012**, *101*, 053123.
(33) Kocabas, C.; Dunham, S.; Cao, Q.; Cimino, K.; Ho, X.; Kim, H. S.; Dawson, D.; Payne, J.; Stuenkel, M.; Zhang, H.; Banks, T.; Feng, M.; Rotkin, S. V.; Rogers, J. A. High-Frequency Performance of Submicrometer Transistors That Use Aligned Arrays of Single-Walled Carbon Nanotubes. *Nano Lett.* **2009**, *9*, 1937−1943.
(34) Wang, Z.; Liang, S.; Zhang, Z.; Liu, H.; Zhong, H.; Ye, L. H.; Wang, S.; Zhou, W.; Liu, J.; Chen, Y.; Zhang, J.; Peng, L. M. Scalable Fabrication of Ambipolar Transistors and Radio-Frequency Circuits Using Aligned Carbon Nanotube Arrays. *Adv. Mater.* **2014**, *26*, 645−652.
(35) Hu, Y.; Kang, L.; Zhao, Q.; Zhong, H.; Zhang, S.; Yang, L.; Wang, Z.; Lin, J.; Li, Q.; Zhang, Z.; Peng, L.; Liu, Z.; Zhang, J. Growth of High-Density Horizontally Aligned Swnt Arrays Using Trojan Catalysts. *Nat. Commun.* **2015**, *6*, 6099.
(36) Cao, Y.; Che, Y.; Gui, H.; Cao, X.; Zhou, C. Radio Frequency Transistors Based on Ultra-High Purity Semiconducting Carbon Nanotubes with Superior Extrinsic Maximum Oscillation Frequency. *Nano Res.* **2016**, *9*, 363−371.
(37) Wang, Z. X.; Ding, L.; Pei, T. A.; Zhang, Z. Y.; Wang, S.; Yu, T.; Ye, X. F.; Peng, F.; Li, Y.; Peng, L. M. Large Signal Operation of Small Band-Gap Carbon Nanotube-Based Ambipolar Transistor: A High-Performance Frequency Doubler. *Nano Lett.* **2010**, *10*, 3648−3655.
(38) Wang, Z. X.; Zhang, Z. Y.; Zhong, H.; Pei, T.; Liang, S. B.; Yang, L. J.; Wang, S.; Peng, L. M. Carbon Nanotube Based Multifunctional Ambipolar Transistors for AC Applications. *Adv. Funct. Mater.* **2013**, *23*, 446−450.
(39) Wang, Z. X.; Liang, S. B.; Zhang, Z. Y.; Liu, H. G.; Zhong, H.; Ye, L. H.; Wang, S.; Zhou, W. W.; Liu, J.; Chen, Y. B.; Zhang, J.; Peng, L. M. Scalable Fabrication of Ambipolar Transistors and Radio-Frequency Circuits Using Aligned Carbon Nanotube Arrays. *Adv. Mater.* **2014**, *26*, 645−652.
(40) Che, Y.; Wang, C.; Liu, J.; Liu, B.; Lin, X.; Parker, J.; Beasley, C.; Wong, H. S.; Zhou, C. Selective Synthesis and Device Applications of Semiconducting Single-Walled Carbon Nanotubes Using Isopropyl Alcohol as Feedstock. *ACS Nano* **2012**, *6*, 7454−7462.
(41) Kocabas, C.; Hur, S. H.; Gaur, A.; Meitl, M. A.; Shim, M.; Rogers, J. A. Guided Growth of Large-Scale, Horizontally Aligned Arrays of Single-Walled Carbon Nanotubes and Their Use in Thin-Film Transistors. *Small* **2005**, *1*, 1110−1116.
(42) Li, J.; Liu, K.; Liang, S.; Zhou, W.; Pierce, M.; Wang, F.; Peng, L.; Liu, J. Growth of High-Density-Aligned and Semiconducting-Enriched Single-Walled Carbon Nanotubes: Decoupling the Conflict between Density and Selectivity. *ACS Nano* **2014**, *8*, 554−562.
(43) Liu, X. L.; Han, S.; Zhou, C. W. Novel Nanotube-on-Insulator (NOI) Approach toward Single-Walled Carbon Nanotube Devices. *Nano Lett.* **2006**, *6*, 34−39.
(44) Arnold, M. S.; Green, A. A.; Hulvat, J. F.; Stupp, S. I.; Hersam, M. C. Sorting Carbon Nanotubes by Electronic Structure Using Density Differentiation. *Nat. Nanotechnol.* **2006**, *1*, 60−65.
(45) Hersam, M. C. Progress Towards Monodisperse Single-Walled Carbon Nanotubes. *Nat. Nanotechnol.* **2008**, *3*, 387−394.
(46) Gerstel, P.; Klumpp, S.; Hennrich, F.; Poschlad, A.; Meded, V.; Blasco, E.; Wenzel, W.; Kappes, M. M.; Barner-Kowollik, C. Highly Selective Dispersion of Single-Walled Carbon Nanotubes *via* Polymer Wrapping: A Combinatorial Study *via* Modular Conjugation. *ACS Macro Lett.* **2014**, *3*, 10−15.
(47) Chen, F. M.; Wang, B.; Chen, Y.; Li, L. J. Toward the Extraction of Single Species of Sinale-Walled Carbon Nanotubes Using Fluorene-Based Polymers. *Nano Lett.* **2007**, *7*, 3013−3017.
(48) Ouyang, M.; Huang, J. L.; Lieber, C. M. Fundamental Electronic Properties and Applications of Single-Walled Carbon Nanotubes. *Acc. Chem. Res.* **2002**, *35*, 1018−1025.
(49) Brady, G. J.; Joo, Y.; Wu, M. Y.; Shea, M. J.; Gopalan, P.; Arnold, M. S. Polyfluorene-Sorted, Carbon Nanotube Array Field-Effect Transistors with Increased Current Density and High On/Off Ratio. *ACS Nano* **2014**, *8*, 11614−11621.

DOI: 10.1021/acsnano.6b02395
ACS Nano XXXX, XXX, XXX−XXX

(50) Joo, Y.; Brady, G. J.; Arnold, M. S.; Gopalan, P. Dose-Controlled, Floating Evaporative Self-Assembly and Alignment of Semiconducting Carbon Nanotubes from Organic Solvents. *Langmuir* **2014**, *30*, 3460−3466.
(51) Brady, G. J.; Joo, Y.; Singha Roy, S.; Gopalan, P.; Arnold, M. S. High Performance Transistors *via* Aligned Polyfluorene-Sorted Carbon Nanotubes. *Appl. Phys. Lett.* **2014**, *104*, 083107.
(52) Badmaev, A.; Che, Y.; Li, Z.; Wang, C.; Zhou, C. Self-Aligned Fabrication of Graphene RF Transistors with T-Shaped Gate. *ACS Nano* **2012**, *6*, 3371−3376.
(53) Cao, Q.; Han, S. J.; Tulevski, G. S.; Franklin, A. D.; Haensch, W. Evaluation of Field-Effect Mobility and Contact Resistance of Transistors That Use Solution-Processed Single-Walled Carbon Nanotubes. *ACS Nano* **2012**, *6*, 6471−6477.
(54) Lin, Y. M.; Dimitrakopoulos, C.; Jenkins, K. A.; Farmer, D. B.; Chiu, H. Y.; Grill, A.; Avouris, P. 100-GHz Transistors from Wafer-Scale Epitaxial Graphene. *Science* **2010**, *327*, 662−662.
(55) Han, S. J.; Garcia, A. V.; Oida, S.; Jenkins, K. A.; Haensch, W. Graphene Radio Frequency Receiver Integrated Circuit. *Nat. Commun.* **2014**, *5*, 3086.
(56) Guo, Z. L.; Dong, R.; Chakraborty, P. S.; Lourenco, N.; Palmer, J.; Hu, Y. K.; Ruan, M.; Hankinson, J.; Kunc, J.; Cressler, J. D.; Berger, C.; de Heer, W. A. Record Maximum Oscillation Frequency in C-Face Epitaxial Graphene Transistors. *Nano Lett.* **2013**, *13*, 942−947.
(57) Cheng, R.; Jiang, S.; Chen, Y.; Liu, Y.; Weiss, N.; Cheng, H. C.; Wu, H.; Huang, Y.; Duan, X. F. Few-Layer Molybdenum Disulfide Transistors and Circuits for High-Speed Flexible Electronics. *Nat. Commun.* **2014**, *5*, 5143.
(58) Wang, H.; Wang, X.; Xia, F.; Wang, L.; Jiang, H.; Xia, Q.; Chin, M. L.; Dubey, M.; Han, S. J. Black Phosphorus Radio-Frequency Transistors. *Nano Lett.* **2014**, *14*, 6424−6429.

DOI: 10.1021/acsnano.6b02395
ACS Nano XXXX, XXX, XXX−XXX